



CrossMark
 click for updates

Cite this: *RSC Adv.*, 2015, 5, 38264

An efficient and reusable catalyst for Suzuki cross-coupling reactions in aqueous solution—hollow palladium–ferrum bimetallic magnetic spheres

Mengmeng Liu, Xiaohang Zhu, Li Wu, Xingchun Zhou, Jing Li and Jiantai Ma*

Hollow Pd–Fe bimetallic magnetic spheres are synthesized in this work. Such materials are successfully characterized by ICP-AES, XPS, TEM, BET, XRD, and VSM, etc. These as-prepared hollow materials have high catalytic activity during Suzuki cross-coupling reactions between aryl halides and arylboronic acids in water. Meanwhile, the catalytic activity can be adjusted *via* changing the composition of the catalyst. The enhanced activity was attributed to both the hollow chamber structure and the promotional effect of Fe-dopants, which provided more Pd active sites during the reaction. Besides, due to the incorporation of ferrum, the recycling processes of the magnetic catalyst became simpler and more efficient.

Received 4th December 2014
 Accepted 20th April 2015

DOI: 10.1039/c4ra15775c

www.rsc.org/advances

Introduction

Suzuki cross-coupling reactions have received remarkable scientific attention over the past few decades.¹ The palladium-catalyzed Suzuki cross-coupling reaction between aryl halides and arylboronic acids is one of the most effective methods for carbon–carbon bond formation. Such a reaction has been employed in the synthesis of biaryl compounds which are important moieties in many natural products, pharmaceuticals and functional materials.^{2–8} In comparison with many other cross-coupling reactions, the Suzuki reaction has practical advantages, since well-tolerated and functionalized arylhalides react with innocuous boronic acids.⁹ Generally, these reactions are catalyzed by homogeneous palladium salts with various ligands in organic solvents. Recently, Suzuki cross-coupling reactions have shown relatively high activity and selectivity in aqueous media as well.^{10–13} However, the separation and recovery of homogeneous catalysts from products and reaction media are difficult, which are the key issues for sustainable development of the chemical industry. Thus, more research has been focused on the preparation of heterogeneous catalyst for Suzuki reaction. Much of the heterogeneous palladium-based catalysts are prepared by immobilizing or stabilizing Pd nanospheres on different supports, such as carbon nanotubes,¹⁴ metal oxides,¹⁵ polymers,¹⁶ double hydroxides,¹⁷ high surface-area silica^{18,19} and magnetic nanomaterials.^{20,21} Unfortunately, there are some disadvantage of these catalysts, such as: (i) the active sites of these catalysts are not well accessible in the reactions; (ii) the contact between reactants and active sites of catalysts is often poor; (iii) the tiny Pd nanoparticles also agglomerate due to high surface energy.

At present, there has been growing interests in the hollow materials with tunable chamber, because of the high surface area, low density, easy recovery, self-supporting capacity, cost reduction, and surface permeability.^{22–26} With those properties, hollow materials may play a promising role in many application, such as catalysis, adsorption, microelectronics, and photonics, etc.^{27–30} Pd nanospheres catalyst with a hollow chamber has been successfully synthesized and the catalyst showed high catalytic activity in liquid-phase phenol hydrogenation reaction.^{31,32} Because of the high cost of Pd, economizing expensive Pd metal in the catalyst is required in the industrial production. Design and synthesis of Pd/non-noble-metal catalysts is also a promising way to reduce the palladium content in the catalyst.³⁰ It is facile to prepare new materials with a controllable shape and morphology by using the vesicle-assistance, as vesicle templates with diverse structures can be easily built up in the liquid-crystal phase and removed from the final products by washing.³³

In this paper, we report the synthesis of a novel mesoporous Pd–Fe alloy magnetic spheres catalyst with a hollow chamber, using a vesicle template of tetrabutylphosphonium bromide (Bu₄PBr). This catalyst shows high activity during the Suzuki reactions, due to its unique structure. Furthermore, the catalytic activity of hollow Pd–Fe spheres can be tuned by controlling the ratio of Pd to Fe. Due to the participation of ferrum, recycling process of magnetic catalyst has also become simpler and more efficient.

Experimental

Catalyst preparation

All of the chemicals used in this experiment were of analytical grade and used without further purification. The hollow Pd–Fe catalysts were prepared according to the procedure described as

College of Chemistry and Chemical Engineering, Lanzhou University, Lanzhou 730000, P. R. China. E-mail: majiantai@lzu.edu.cn; Fax: +86 931 8912311; Tel: +86 931 8912311

follows: first, an aqueous solution of Bu_4PBr (100 mL, 0.010 M) was added into another aqueous solution composed of PdCl_2 (5 mL, 0.020 M) and an appropriate amount of $\text{FeCl}_3 \cdot 6\text{H}_2\text{O}$ (0.020 M). The mixture was stirred vigorously for 30 min to form a turbid solution. Then, an appropriate amount of NaBH_4 aqueous solution (4.0 M) was added dropwisely into the turbid solution under vigorous stirring at 30 °C. After reaction was completed, the black precipitate was washed free from Cl^- or Na^+ ions with deionized water until a $\text{pH} = 7$ was achieved, and dried under vacuum. The molar ratio of $\text{B}/(\text{Pd} + \text{Fe})$ was controlled as 10/1 in the reaction to ensure the complete reduction of Pd^{2+} ions. The Fe^- and Pd^- contents in the Pd–Fe samples were adjusted by varying the molar ratio of $\text{Fe}^{3+}/\text{Pd}^{2+}$ in the precursor solution.³⁰ The asprepared Pd–Fe samples in the presence of Bu_4PBr were named as Pd–Fe– $x(\text{H})$ (hollow), with x representing the molar ratio of Fe^{3+} to Pd^{2+} in the precursor solution (Table 1).

Catalyst characterization

Inductive coupled plasma atomic emission spectrometer (ICP–AES) analysis was conducted with Perkin Elmer (Optima-4300DV). A FEI–TECNAI G2 transmission electron microscope operating at 200 kV (FEI company) was used to make the transmission electron microscopy (TEM) images, high resolution TEM (HRTEM) images, high-angle annular dark field scanning transmission electron microscopy (HAADF–STEM) images and element analysis mapping. Elemental composition data was collected by energy dispersive X-ray spectroscopy (EDS) performed using a TECNAI G2 microscope. XRD measurements were carried out at room temperature and performed on a Rigaku D/max-2400 diffractometer using $\text{Cu-K}\alpha$ radiation as the X-ray source in the 2θ range of 10–100°. X-ray photoelectron spectroscopy (XPS) analysis was carried on a PHI-5702 X-ray photoelectron spectrometer. Specific surface areas were calculated by the Brunauer–Emmett–Teller (BET) method and pore sizes by the Barrett–Joyner–Halenda (BJH) methods using Brunauer–Emmett–Teller (Tristar II 3020).

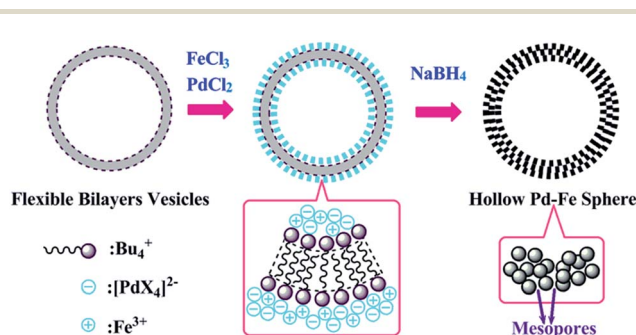
In a typical experiment, aryl halide (1.5 mmol), phenylboronic acids (2.25 mmol) and NaOH (3 mmol) were added to water (5 mL) in a 10 mL round-bottomed flask. Then the catalyst

(containing 0.015 mmol Pd) was added, and the mixture was stirred at 70 °C in air. The reaction process was monitored by thin layer chromatography (TLC). After completion of the reaction, the mixture was cooled to room temperature and separated by external magnetic field, the resultant residual mixture diluted with 10 mL ethyl acetate. The organic fraction was dried over MgSO_4 , and an aliquot was taken with a syringe and subjected to GC or GC–MS analysis. Yields were calculated against the consumption of aryl halides. For the recycling test, the recovered catalyst was further washed sufficiently with ethanol and water before dried at room temperature for the next cycle.

Results and discussion

Structural characteristics

The preparation of Pd–Fe– $x(\text{H})$ bimetallic spheres is based on a vesicle-assisted chemical reduction method, which is schematically described in Scheme 1. Firstly, the Bu_4PBr in water may be dissociated into Br^- and Bu_4P^+ ions. Then, the Br^- can coordinate with Pd^{2+} to form $[\text{PdX}_4]^{2-}$, which induces the rapid coassembly with Bu_4P^+ into spherical vesicles.³³ The $[\text{PdX}_4]^{2-}$ and Fe^{3+} surround the outer shell of the vesicles due to electrostatic interactions. Subsequently, Pd(II) ions and Fe(III) can be reduced into metallic Pd nanoparticles and Fe nanoparticles by adding BH_4^- , which forms a thin shell surrounding the vesicle



Scheme 1 The possible formation process of hollow Pd–Fe spheres; X = Cl or Br.

Table 1 Composition and catalytic properties of the as-prepared Pd–Fe– $x(\text{H})$ catalysts^a

Catalyst	Nominal composition (atom%)	Bulk composition (atom%)	Yield ^b (%)
Pd–Fe–0.5(H)	Pd : Fe = 2 : 1	Pd : Fe = 64 : 36	90
Pd–Fe–1(H)	Pd : Fe = 1 : 1	Pd : Fe = 48 : 52	99
Pd–Fe–2(H)	Pd : Fe = 1 : 2	Pd : Fe = 33 : 67	93
Pd–Fe–3(H)	Pd : Fe = 1 : 3	Pd : Fe = 24 : 76	94
Pd–Fe–5(H)	Pd : Fe = 1 : 5	Pd : Fe = 16 : 84	95

^a Reaction conditions: a catalyst amount containing 0.015 mmol Pd, aryl halides (1.5 mmol), phenylboronic acids (2.25 mmol), sodium hydroxide (3 mmol) and water (5.0 mL), reaction time, 50 min, $T = 70$ °C. ^b Determined by GC or GC–MS.

templates.^{33,34} Finally, hollow Pd–Fe spheres are obtained after washing out the vesicle template.³⁵

According to ICP-AES analysis, it is found that the compositions of Pd and Fe in all Pd–Fe–*x*(H) samples are very similar to those in the precursor solution (see Table 1).

XPS spectroscopy was performed to determine the oxidation state of surface elements in the Pd–Fe–1(H) composites. The main doublet peak in XPS spectrum could be attributed to Pd 3d as shown in Fig. 1a. The binding energy of the doublet peaks at 335.35 eV (assigned to Pd⁰ 3d_{5/2}) and 340.70 eV (assigned to Pd⁰ 3d_{3/2}) indicate that all Pd atoms are present in the Pd⁰ state. Compared with 334.55 eV and 339.75 eV for pure Pd nanoparticles, as light change in the electronic properties of Pd is indicated by small shifts to higher energy, which also confirms the formation of alloys.³⁶ Additionally, two types of Fe species are detected (Fig. 1b): Fe⁰ (Fe 2p_{3/2} located at 705.55 eV) and oxidized Fe (Fe 2p_{3/2} located at 711.79 eV). However, it is still unclear whether these oxidized Fe species are from the oxidation of iron during or after the synthesis process.

The morphologies and structural features of the hollow Pd–Fe–1(H) bimetallic spheres can be observed directly from the TEM images (Fig. 2). The as-synthesized spherical particles are very uniform in size and the average diameter is about 100 nm. TEM observation further confirms the hollow structure of the spheres with outer shells, and the thickness of the outer shells is about 10 nm. To investigate each element's distribution in the Pd–Fe bimetal further, high-angle annular dark-field scanning

transmission electron microscope energy dispersive X-ray spectroscopy images are presented (Fig. 3). Cross-sectional compositional line profiles (Fig. 3d) demonstrate the hollow structures and homogenous distribution of the Pd–Fe bimetal. The mapping results (Fig. 3b and c) indicates the uniform distribution of Pd (blue) and Fe (yellow) in the outer shells of the hollow spheres as well.

Pd–Fe–1(H) displayed type-IV adsorption/desorption isotherms with a hysteresis loop in BET experiments, indicative of mesoporous character (Fig. 4). This is also consistent with the high-magnification TEM image (Fig. 3a), which showed wormhole-like mesopores in the outer shell. SBET of Pd–Fe–1(H) was determined to be 84.77 m² g⁻¹. The above results confirmed the formation of the hollow structure and the mesoporous shells.

Pd–Fe bimetal crystallized well and showed obvious lattice structure in the high-resolution transmission electron microscopy (HRTEM) image in Fig. 5. Meanwhile, the inset SAED pattern of Pd–Fe–1(H) in Fig. 5 shows diffuse rings resulted from the Pd (111), (200), (220) and (311) reflections.³⁷ This is consistent with the X-ray diffraction (XRD) pattern, as the fcc Pd (111), (311) diffractions and Pd–Fe (200), (220) diffractions matched with Pd–Fe alloy standard card (PDF. 00-002-1440)

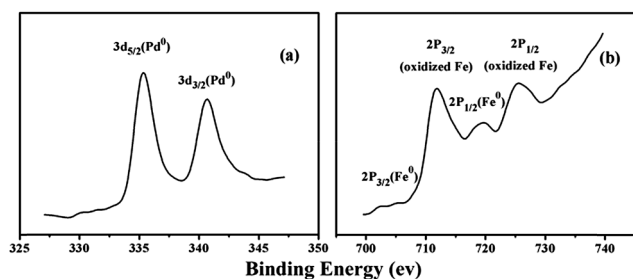


Fig. 1 XPS spectra of Pd–Fe–1(H). (a) Pd 3d_{5/2} and 3d_{3/2} peaks, and (b) Fe 2p_{3/2} and 2p_{1/2} peaks.

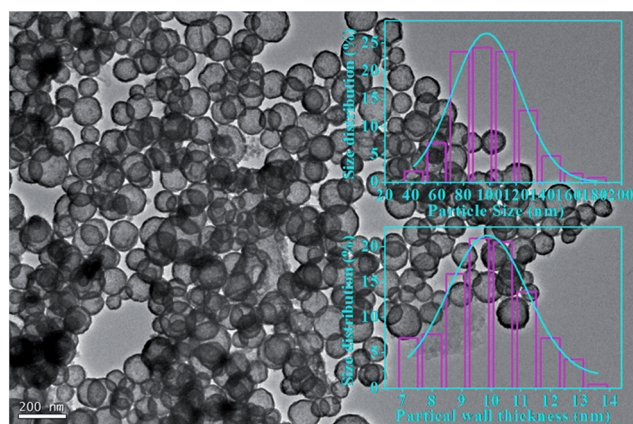


Fig. 2 TEM images of Pd–Fe–1(H).

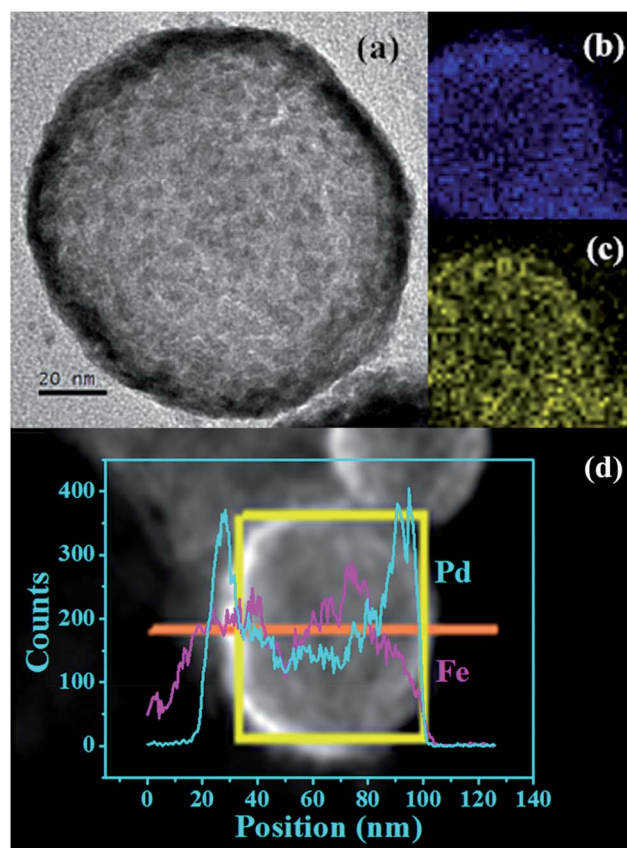


Fig. 3 (a) TEM image of a single hollow sphere in Pd–Fe–1(H), (b and c) elemental mapping data [Pd (blue) and Fe (yellow)] for the sphere in (a). (d) Cross-sectional compositional line profiles taken from Pd–Fe–1(H) spheres (the background shows the HAADFSTEM image of a single hollow sphere in Pd–Fe–1(H)).

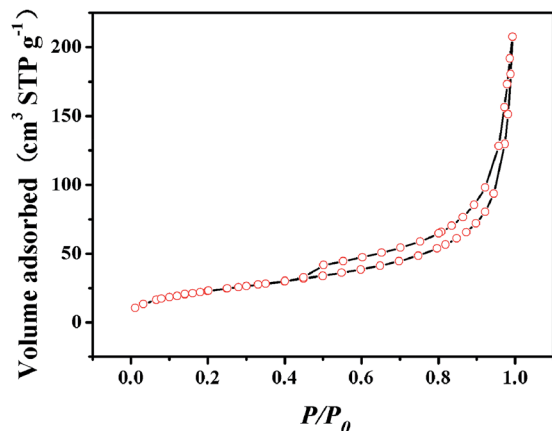


Fig. 4 N₂ adsorption/desorption isotherms of Pd-Fe-1(H).

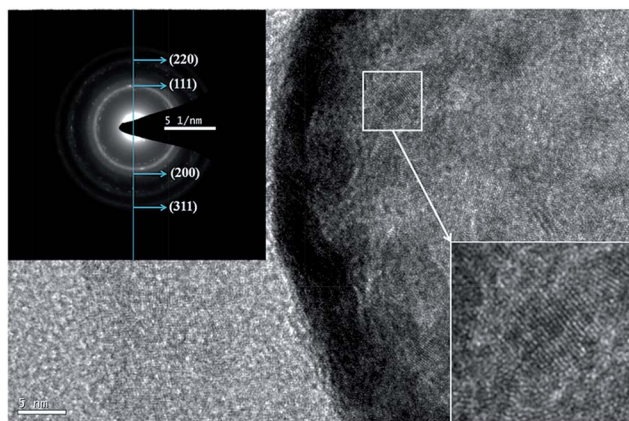


Fig. 5 HRTEM image of Pd-Fe-1(H). The inset is the SAED image of Pd-Fe-1(H).

(Fig. 6). Then the Joint Committee Powder Diffraction Standard (JCPDS) of Fe (PDF. 00-001-1252) and Pd (PDF. 00-001-1201) are used for comparison. The diffraction peaks of Pd-Fe-1(H) are shifted to the position between those of the two pure metals, which further confirms alloy formation.³⁸

Magnetic measurements were carried out on a vibrating sample magnetometer (VSM) at room temperature. The superpara magnetic behavior of the magnetic Pd-Fe-1(H) was demonstrated by plotting magnetization curves (Fig. 7). There was no hysteresis in the magnetization for the tested particles. Furthermore, it was observed that the superpara magnetic behaviour of the magnetic particles and the value of the saturation magnetization was 5.68 emu g⁻¹ for Pd-Fe-1(H), which represents its excellent magnetism. Thus, our catalyst can be recovered from the solution with the help of external magnetic field. Meanwhile, the figure also shows the photograph of the catalyst being pulled magnetically.

Catalyst testing for Suzuki coupling reactions

After the successful preparation of Pd-Fe-*x*(H), its effectiveness for the Suzuki coupling reaction between iodobenzene and

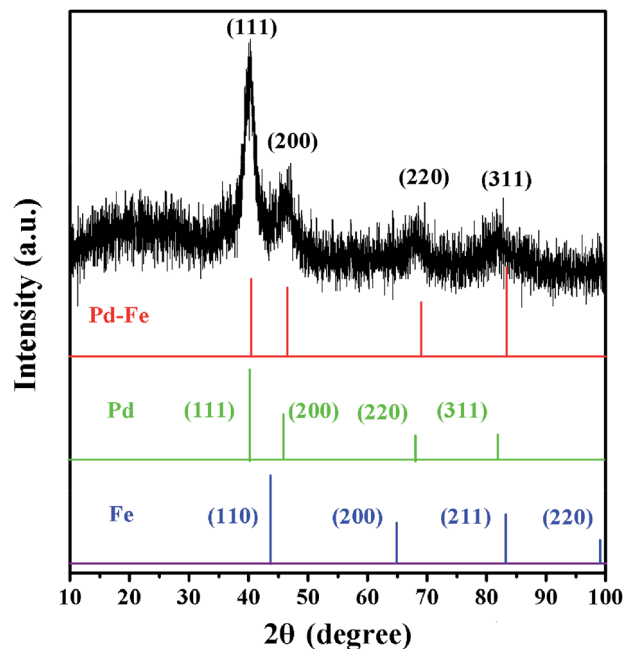


Fig. 6 XRD patterns of Pd-Fe-1(H).

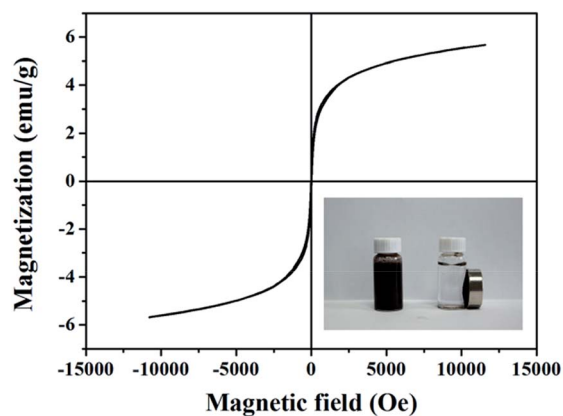
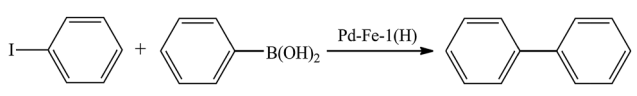


Fig. 7 Room temperature magnetization curves of Pd-Fe-1(H).

phenylboronic acids in water was examined using the same amount of Pd in the reaction mixtures. It could be clearly observed that the iodobenzene conversion over Pd-Fe-*x*(H) was firstly increased and then decreased with the increase of Fe-content (Table 1). The maximum iodobenzene conversion was obtained on Pd-Fe-1(H). The promotional effect of Fe-dopants on catalytic activity should be attributed to their dispersing effect on Pd active sites, which would allow more favorable oxidative addition of the metallic Pd to the carbon-halogen bond, enhancing the catalytic efficiency.³⁹ However, excess amount of Fe-content was detrimental to the activity because of the coverage of Pd active sites. At the same time, when the Pd content is too high, it will make the agglomeration of Pd particles and the decrease of the catalytic activity.

The reaction between iodobenzene and phenylboronic acid was used as a model reaction for the optimization of alkaline

Table 2 The cross-coupling of phenylboronic acid and iodobenzene with different base and indifferent temperature in the presence of the Pd-Fe-1(H) catalyst^a

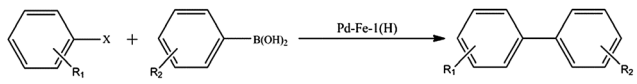


Entry	Base	Temperature (°C)	Yield ^b (%)
1	Na ₂ CO ₃	70	21
2	K ₂ CO ₃	70	77
3	K ₃ PO ₄ ·3H ₂ O	70	76
4	KOH	70	84
5	NaOH	70	94
6	NaOH	60	86
7	NaOH	80	99

^a Reaction conditions: a catalyst amount containing 0.015 mmol Pd, aryl halides (1.5 mmol), phenylboronic acids (2.25 mmol), water (5.0 mL) and base (3 mmol), reaction time = 30 min. ^b Determined by GC or GC-MS.

and temperature in Suzuki reaction. The results were summarized in Table 2. With the temperature fixed as 70 °C, the reaction proceeded well (yield is 94%) when the inorganic base NaOH was used. As NaOH was the most efficient base for the present catalytic system, it was chosen for subsequent

Table 3 Pd-Fe-1(H) catalyzed Suzuki coupling reaction^a



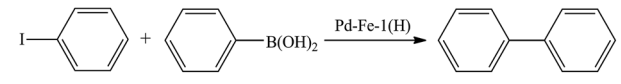
Entry	R ₁	X	R ₂	T	Yield ^b (%)	Ton	Tof (h ⁻¹)
1	4-H	I	4-H	30 min	94	63	126
2	4-H	I	4-H	50 min	99	66	79.2
3	4-CH ₃	I	4-H	3 h	96	64	21.3
4	4-OCH ₃	I	4-H	2 h	96	64	32
5	4-OH	I	4-H	3 h	95	63.3	21.8
6	4-COCH ₃	I	4-H	50 min	98	65.3	78.4
7	2-NH ₂	I	4-H	2 h	95	63.3	32.7
8	4-H	Br	4-H	8.5 h	93	62	7.3
9	4-H	Br	4-H	9.5 h	97	64.7	6.8
10	4-CH ₃	Br	4-H	20 h	75	50	2.5
11	4-NH ₂	Br	4-H	18 h	98	65.3	3.6
12	4-COCH ₃	Br	4-H	2 h	98	65.3	32.7
13	-NO ₂	Br	4-H	2 h	98	65.3	32.7
14	2-NO ₂	Br	4-H	9 h	50	33.3	3.7
15 ^c	2-NO ₂	Br	4-H	9 h	98	65.3	7.3
16	4-H	Cl	4-H	20 h	49	32.7	1.6
17	4-CH ₃	Cl	4-H	24 h	45	30	1.3
18	4-H	I	4-CH ₃	2 h	95	63.3	31.7
19	4-H	Br	4-CH ₃	11 h	94	63	5.7
20	4-H	Cl	4-CH ₃	23 h	51	34	1.5

^a Reaction conditions: a catalyst amount containing 0.015 mmol Pd, aryl halides (1.5 mmol), phenylboronic acids (2.25 mmol), sodium hydroxide (3 mmol) and water (5.0 mL), T = 70 °C. ^b Determined by GC or GC-MS. ^c TBAB (1 mmol).

investigations. Further experiments showed that when the temperature increased from 60 °C to 70 °C, the yield of product was increased from 86% to 94% (Table 3, entries 5–7). However, when the temperature was 80 °C, the yield of product did not increase significantly. Therefore, considering energy saving, the optimized reaction condition is: 70 °C and NaOH.

The results of the Suzuki cross-coupling reaction of aryl halides with phenylboronic acid or 4-methylphenylboronic acid are summarized in Table 3. At a Pd loading of 1 mol%, Pd-Fe-1(H) afforded satisfactory biaryl yields (95–99%) for iodobenzene containing 4-CH₃, 4-OCH₃, 4-OH, 4-COCH₃ and 2-NH₂ groups in the time range from 50 min to 3 h (Table 3, entries 2–7). For aryl bromides with substituents such as 4-CH₃, 4-NH₂, 4-COCH₃, 4-NO₂ and 2-NO₂, complete conversions were observed and the corresponding biaryl products with yields of 50–98% were also achieved in the time range from 2 h to 20 h (Table 3, entries 8–15). Aryl bromides bearing strong electron-withdrawing groups need relatively longer time to produce a moderate yield. Further studies indicated that chlorobenzene can also react with phenylboronic acid. However, it took a very long time even more than 20 h to achieve a good yield of 45–49% (Table 3, entries 16–17). Pd-Fe-1(H) also exhibited a high activity in the Suzuki cross-

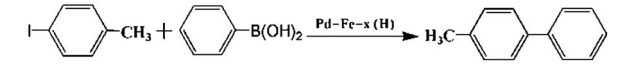
Table 4 Reusability of the hollow Pd-Fe-1(H) catalyst for the Suzuki reaction^a



Run	1	2	3	4	5
Yield after 50 min ^b (%)	99	96	95	93	90
Run	6	7	8	9	10
Yield after 50 min ^b (%)	90	88	89	86	85

^a Reaction conditions: a catalyst amount containing 0.015 mmol Pd, aryl halides (1.5 mmol), phenylboronic acids (2.25 mmol), sodium hydroxide (3 mmol) and water (5.0 mL), reaction time = 50 min, T = 70 °C. ^b Determined by GC or GC-MS.

Table 5 Catalytic activity of different proportion of Pd-Fe-x(H)^a



Catalyst	Yield ^b (%)	Yield ^b (%) after 5 times
Pd-Fe-0.5(H)	87	80
Pd-Fe-1(H)	96	90
Pd-Fe-2(H)	89	81
Pd-Fe-3(H)	90	83
Pd-Fe-5(H)	91	85

^a Reaction conditions: a catalyst amount containing 0.015 mmol Pd, 4-iodotoluene (1.5 mmol), phenylboronic acids (2.25 mmol), sodium hydroxide (3 mmol) and water (5.0 mL), reaction time, 3 h, T = 70 °C. ^b Determined by GC or GC-MS.

coupling reactions of 4-methylphenylboronic acid, with satisfactory yields of 51–95% (Table 3, entries 18–20).

The recyclability of Pd–Fe–1(H) was further investigated because the recyclability of the Suzuki catalyst is one of the most important issues for practical applications. We therefore turned our attention to the reusability of our Pd catalyst using phenylboronic acid and iodobenzene as model substrates (Table 4). After the model Suzuki coupling reaction was carried out under the optimized reaction conditions, the catalyst was recovered by external magnetic separation, washed with ethanol completely, dried under vacuum and reused for the next run. As shown in Table 4, no significant decrease in conversion was observed after performing at least 10 cycle experiments. ICP analysis detected that the weight loss of Pd after 10 consecutive runs is 2.1%. A small amount of yield decline may be due to the loss of Pd nanoparticles in the recycling process. It is thus concluded that the nature of Pd active sites did not change after being used repetitively. The results further confirmed the high recyclability of Pd–Fe–1(H).

Suzuki coupling reactions between 1-iodo-4-methylbenzene and phenylboronic acids in aqueous medium were used for template reaction. We conducted a series of experiments, the datum refer to Table 5. All the Pd–Fe catalysts displayed high catalytic activity and the yield could reach above 80% after cycle 5 times. Especially when Pd : Fe = 1 : 1, it could achieve a good yield of 90% which was much better than others and the reduction of the yield was least. The above conclusions fully indicate that Pd–Fe–1(H) has optimal catalytic activity.

Conclusions

In summary, the present work reports composition controllable and easily reusable Pd–Fe catalysts with hollow chamber structure prepared through a vesicle-assisted chemical reduction method. The as-prepared hollow Pd–Fe catalyst exhibits much high activity during Suzuki cross-coupling reactions in water by increasing the number of Pd active sites. Other hollow bimetallic catalysts could also be prepared based on the present method, offering more opportunities in designing new and powerful catalysts.

Acknowledgements

The authors are grateful to the Key Laboratory of Nonferrous Metals Chemistry and Resources Utilization, Gansu Province, for financial support. Additionally, we are also very grateful for the Scholarship Award for Excellent Doctoral Student granted by Lanzhou University. The authors are grateful to Dr R. Q. Wang for correction of the manuscript.

Notes and references

- N. Miyaura, K. Yamada and A. Suzuki, *Tetrahedron Lett.*, 1979, **20**, 3437.
- A. Molnar, *Chem. Rev.*, 2011, **111**, 2251.
- V. Polshettiwar, A. Decottignies, C. Len and A. Fihri, *ChemSusChem*, 2010, **3**, 502.
- R. Narayanan, *Molecules*, 2010, **15**, 2124.
- M. Kertesz, C. H. Choi and S. Yang, *Chem. Rev.*, 2005, **105**, 3448.
- R. Capdeville, E. Buchdunger, J. Zimmermann and A. Matter, *Nat. Rev. Drug Discovery*, 2002, **1**, 493.
- H. Tomori, J. M. Fox and S. L. Buchwald, *J. Org. Chem.*, 2000, **65**, 5334.
- S. Lightowler and M. Hird, *Chem. Mater.*, 2005, **17**, 5538.
- Q. Xiao, S. Sarina, E. Jaatinen, J. F. Jia, D. P. Arnold, H. W. Liu and H. Y. Zhu, *Green Chem.*, 2014, **16**, 4272.
- N. Miyaura, T. Yanagi and A. Suzuki, *Synth. Commun.*, 1981, **11**, 513.
- L. Wu, Z. Li, F. Zhang, Y. He and Q. Fan, *Adv. Synth. Catal.*, 2008, **350**, 846.
- K. Sawai, R. Tatumi, T. Nakahodo and H. Fujihara, *Angew. Chem., Int. Ed.*, 2008, **47**, 7023.
- V. Polshettiwar, A. Decottignies, C. Len and A. Fihri, *ChemSusChem*, 2010, **3**, 502.
- V. I. Sokolov, E. G. Rakov, N. A. Bumagin and M. G. Vinogradov, *Fullerenes, Nanotubes, Carbon Nanostruct.*, 2010, **18**, 558–563.
- A. Gniewek, J. J. Ziolkowski, A. M. Trzeciak, M. Zawadzki, H. Grabowska and J. Wrzyszczyk, *J. Catal.*, 2008, **254**, 121–130.
- R. Najman, J. K. Cho, A. F. Coffey, J. W. Davies and M. Bradley, *Chem. Commun.*, 2007, 5031–5033.
- S. Y. Liu, Q. Z. Zhou, Z. N. Jin, H. J. Jiang and X. Z. Jiang, *Chin. J. Catal.*, 2010, **31**, 557–561.
- Z. Zheng, H. Li, T. Liu and R. Cao, *J. Catal.*, 2010, **270**, 268–274.
- D. D. Das and A. Sayari, *J. Catal.*, 2007, **246**, 60–65.
- S. E. Garcia-Garrido, J. Francos, V. Cadierno, J. M. Basset and V. Polshettiwar, *ChemSusChem*, 2011, **4**, 104–111.
- V. Polshettiwar and R. S. Varma, *Tetrahedron*, 2010, **66**, 1091–1097.
- Y. Li, P. Zhou, Z. Dai, Z. Hu, P. Sun and J. C. Bao, *New J. Chem.*, 2006, **30**, 832.
- P. Zhou, Y. Li, P. Sun, J. Zhou and J. C. Bao, *Chem. Commun.*, 2007, 1418.
- G. Chen, D. Xia, Z. Nie, Z. Wang, L. Wang, L. Zhang and J. Zhang, *Chem. Mater.*, 2007, **19**, 1840.
- X. Chen, W. Yang, S. Wang, M. Qiao, S. Yan, K. Fan and H. He, *New J. Chem.*, 2005, **29**, 266.
- H. Li, D. Q. Zhang, G. S. Li, Y. Xu, Y. F. Lu and H. X. Li, *Chem. Commun.*, 2010, **46**, 791.
- Y. Sun, B. Mayers and Y. Xia, *Adv. Mater.*, 2003, **15**, 641.
- Y. Song, R. M. Garcia, R. M. Dorin, H. Wang, Y. Qiu and J. A. Shelnut, *Angew. Chem., Int. Ed.*, 2006, **45**, 8126.
- H. Xu and W. Wang, *Angew. Chem., Int. Ed.*, 2007, **46**, 1489.
- H. Li, Z. H. Zhu, J. Liu, S. H. Xie and H. X. Li, *J. Mater. Chem.*, 2010, **20**, 4366.
- H. Li, J. Liu, S. H. Xie, M. H. Qiao, W. L. Dai, Y. F. Lu and H. X. Li, *Adv. Funct. Mater.*, 2008, **18**, 3235.
- H. P. Liang, H. M. Zhang, J. S. Hu, Y. G. Guo, L. J. Wan and C. L. Bai, *Angew. Chem., Int. Ed.*, 2004, **43**, 1540.
- X. Zhang and D. Li, *Angew. Chem., Int. Ed.*, 2006, **45**, 5971.
- Y. Sun, B. Bayers and Y. Xia, *Adv. Mater.*, 2003, **15**, 641.

- 35 H. Li, J. Liu, S. H. Xie, M. H. Qiao, W. L. Dai, Y. F. Lu and H. X. Li, *Adv. Funct. Mater.*, 2008, **18**, 3235.
- 36 M.-L. Wu, D.-H. Chen and T.-C. Huang, *Langmuir*, 2001, **17**, 3877.
- 37 M. Ganesan, R. G. Freemantle and S. O. Obare, *Chem. Mater.*, 2007, **19**, 3464.
- 38 Y. Vasquez, A. K. Sra and R. E. Schaak, *J. Am. Chem. Soc.*, 2005, **127**, 12504.
- 39 C. S. Consorti, F. R. Flores and J. Dupont, *J. Am. Chem. Soc.*, 2005, **127**, 12054.